Chemical Physics Letters 457 (2008) 303–306

Contents lists available at ScienceDirect

Chemical Physics Letters

journal homepage: www.elsevier.com/locate/cplett

Ion imaging study of IO radical photodissociation: Accurate bond dissociation energy determination

Kristin S. Dooley, Justine N. Geidosch, Simon W. North *

Department of Chemistry, Texas A&M University, P.O. Box 30012, College Station, TX 77842, United States

ARTICLE INFO

Article history:
Received 15 February 2008
In final form 2 April 2008
Available online 6 April 2008

ABSTRACT

We have studied the photodissociation dynamics of expansion-cooled IO radicals at 454.9 nm, corresponding to the $A^2\Pi_{3/2}$–$X^2\Pi_{3/2}$ (1–0) bandhead, using velocity map ion imaging. The radicals were generated using a late-mixing dual-valve photolytic reactor source. Analysis of the $I(^2P_{3/2})$ photofragment speed distribution provides a direct determination of the ground state bond energy of $D_0^0(IO) = 54.9^{+0.2}_{-0.4}$ kcal/mol and a heat of formation 298 K of $\Delta H_f^{298}(IO) = 29.2^{+0.4}_{-0.2}$ kcal/mol.

1. Introduction

Iodine compounds, emitted primarily from marine algae [1], play an important role in the chemistry of the marine boundary layer (MBL) [2]. The photolysis of source compounds yields iodine atoms which subsequently react with O_3 to produce IO radicals. The dominant loss processes for IO radicals in the atmosphere are photolysis, an ozone 'null cycle', and reaction with the species HO_2, IO, BrO and ClO which lead to catalytic ozone loss. Higher oxides of iodine are also thought to be efficient aerosol precursors in the MBL [3]. As a consequence, there have been numerous kinetics studies on IO reactions [4–13] and measurements of the IO absorption spectrum [14–18].

The thermochemistry of IO, surprisingly, has been the subject of some controversy. The need for a reliable IO bond dissociation energy (BDE) is the result of IO reactions that are close to thermoneutral. For example, the IO + BrO reaction has 4 thermodynamically accessible channels [19]

$$\begin{aligned} IO + BrO &\rightarrow Br + OIO & \Delta H &\leqslant 0 \text{ kcal/mol} \\ &\rightarrow Br + I + O_2 & \Delta H &= -4.1 \pm 2.6 \text{ kcal/mol} \\ &\rightarrow I + OBrO & \Delta H &= 5.5 \pm 8.6 \text{ kcal/mol} \\ &\rightarrow IBr + O_2 & \Delta H &= -46.5 \pm 2.6 \text{ kcal/mol} \end{aligned} \quad (1)$$

By comparison, the thermochemistry of the other halogen oxides, ClO and BrO, can be derived from Birge–Sponer [20] extrapolation using the vibronic levels of the bound $A^2\Pi_{3/2}$ state [21]. Since only the lowest 6 vibrational levels are clearly resolved in the IO $A^2\Pi_{3/2}$–$X^2\Pi_{3/2}$ absorption spectrum, due to strong perturbations induced by spin–orbit coupling to low lying repulsive electronic states [22], there is considerable uncertainty associated with a Birge-Sponer extrapolation. Predissociation of the (1–0) band of the $A^2\Pi_{3/2}$ state provides a rigorous upper bound to the ground state bond dissociation (BDE) of <62.8 kcal/mol. Birge-Sponer extrapolation of the lowest 6 vibrational levels in the $A^2\Pi_{3/2}$ state by Vaidya and co-workers yielded a BDE of 43.8 ± 4.6 kcal/mol [23]. Subsequent studies using a similar spectroscopic analysis have reported comparable values [21,24,25]. Phillips and Sugden measured IO emission as a function of temperature in an I_2 seeded H_2/O_2 flame [26]. The results were interpreted in terms of the equilibrium reaction,

$$I + O + M \leftrightarrow IO + M \quad (2)$$

and on the basis of variation of the equilibrium constant with temperature the authors deduced a much higher IO BDE value of 57 ± 6 kcal/mol. Molecular beam scattering measurements of the $O(^3P) + ICl \rightarrow IO + Cl$ reaction yielded a value of 53 ± 3 kcal/mol based on statistical modeling of the product kinetic energy distribution [27]. Subsequent molecular beam studies by Buss et al. recommended a slightly larger value of 55 ± 2 kcal/mol [28,29]. Recently, Peterson et al. reported an IO BDE of 54.2 ± 0.6 kcal/mol based on high-level *ab initio* calculations using both direct methods and employing ionization energies and ion cycles [30]. The authors also reported an experimental value derived from the measured $ClO + IO \rightarrow OClO + I$ reaction enthalpy [31] and an improved value for the OCl-O BDE [32] yielding an IO BDE of 55.3 ± 0.5 kcal/mol in reasonable agreement with calculations. There has also been a recent paper by Kaltsoyannis and Plane that report quantum chemical calculations on various atmospherically relevant iodine containing species including IO [33].

Velocity-map ion imaging is a powerful method for the direct determination of accurate bond dissociation energies [34–36]. Wrede et al. have shown that for jet-cooled closed-shell species, spectroscopic accuracy is possible in the case of IBr. We have recently reported BDE values for the ClO and BrO radicals of 63.45 ± 0.06 kcal/mol and 55.9 ± 0.1 kcal/mol, respectively using photodissociation ion imaging [37]. In the present Letter we extend

* Corresponding author. Fax: +1 979 845 2971.
E-mail address: swnorth@tamu.edu (S.W. North).

0009-2614/$ - see front matter © 2008 Elsevier B.V. All rights reserved.
doi:10.1016/j.cplett.2008.04.009

our studies of halogen oxide photodissociation dynamics to IO which, to our knowledge, has not been investigated using the molecular beam method.

2. Experiment

Experiments were performed using a velocity-map ion-imaging apparatus that has been described in detail elsewhere [38,39]. Briefly, the collimated molecular beam was intersected at 90° by two co-propagating linearly polarized laser beams. The dissociation beam at 454.9 nm, corresponding to the bandhead of the 1–0 transition, was generated using a dye laser (Laser Analytical Systems GmbH LDL-2051) operating with the Exciton dye Coumarin 450 pumped by the third harmonic of a Spectra-Physics Lab 150-10 Nd:YAG laser [40]. The wavelength of the dissociation laser was accurately determined by optogalvanic calibration using Cu–Ne hollow cathode lamp. The probe beam was generated by using the second harmonic output of a Spectra Physics Lab 150-10 Nd:YAG laser to pump a dye laser (Spectra Physics PDL-1) operating on the dye Rhodamine 640 followed by frequency doubling. The iodine atoms $I(^2P_{3/2})$ were probed using 2 + 1 REMPI transitions at 304.67 nm ($5p^2P_{3/2} \rightarrow 6p^2D_{5/2}$) [41]. The I^+ ions were accelerated by velocity mapping ion optics before entering a 50 cm long field-free flight tube co-axial with the molecular beam. The ions were projected on a position-sensitive microchannel plate phosphor assembly gated to detect the mass of interest and a CCD camera acquired images of the phosphor screen which were sent to a computer for analysis. The basis set expansion (pBASEX) method [42] was used in the reconstruction of the 3-D velocity distribution from the ion images.

We have employed a dual-valve photolytic source for the production of IO radicals. A mixture of I_2 and O_3 in Helium, each introduced from separate solenoid valves, was irradiated in a quartz tube (0.1 cm I.D.) by the 248 nm output of an excimer laser (GAM Laser, EX10). Based on the relative cross sections, it is photolysis of ozone which initiates the reactions with only minor contribution from I_2 photolysis. The resulting bimolecular reactions generate IO during the transit time to the nozzle exit. Approximately 30 Torr of O_3 in 760 Torr of He was mixed with 2 Torr of I_2 in 760 Torr of He prior to expansion through the quartz nozzle assembly. The O_3 was trapped over Silica Gel (3–6 mm, Fluka) at −78 °C and was warmed to −35 °C to achieve the desired vapor pressure. The rapid self-reaction of IO radicals requires short transit times which can be achieved by irradiation close to the exit of the quartz nozzle. Details of the source design and kinetic modeling will be presented in a subsequent paper.

3. Results and discussion

The photodissociation of IO at 454.9, corresponding to the $A^2\Pi_{3/2}$–$X^2\Pi_{3/2}$ (1–0) bandhead region, was selected for two reasons. Firstly, the (v',0) bands with v' = 0–5 of the $A^2\Pi_{3/2}$–$X^2\Pi_{3/2}$ transition have been studied using cavity ring-down spectroscopy and the (1–0) band was shown to be strongly predissociated [40]. Newman et al. determined a predissociation lifetime of 0.88 ps implying that the photofragment angular distribution should be highly anisotropic near the bandhead [43]. In addition, the (1–0) band represents a compromise between the higher cross section of the (4–0) band and the increased sensitivity to the available energy closer to threshold.

The upper panel in Fig. 1 shows a typical image (left) and reconstruction (right) arising from the photodissociation laser at 454.9 nm and the probe laser at 304.6 nm with the 248 nm source laser off. Only features consistent with I_2 photodissociation at 454.9 nm and 304.6 nm are observed in the image. The lower panel

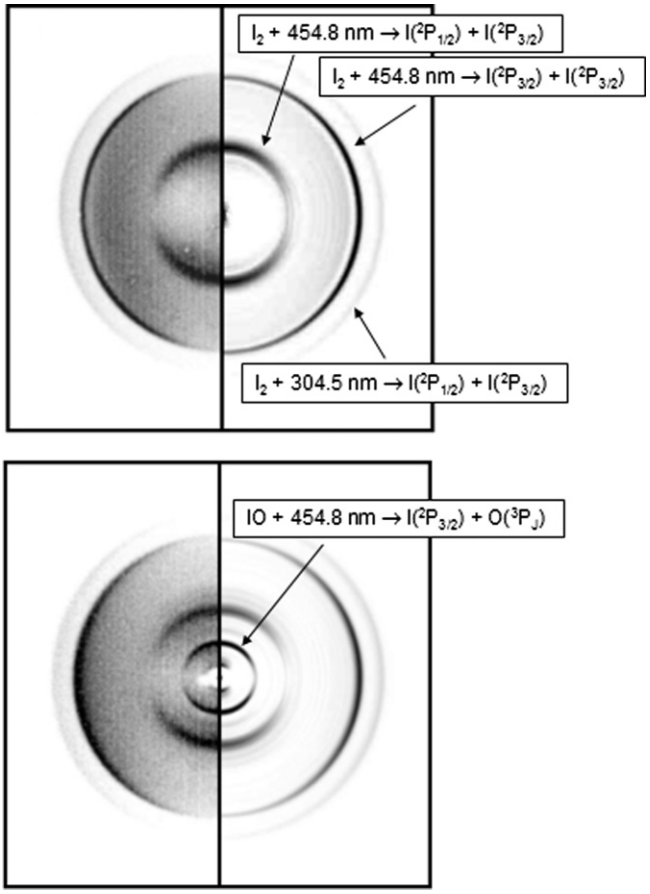

Fig. 1. Upper panel: raw $I(^2P_{3/2})$ ion image (left) and reconstruction (right) collected with the source laser off. Lower panel: raw $I(^2P_{3/2})$ ion image (left) and reconstruction (right) collected with the source laser on.

in Fig. 1 shows raw and reconstructed $I(^2P_{3/2})$ images with the 248 nm source laser on. An additional ring, corresponding to 454.9 nm photodissociation of IO to yield the $I(^2P_{3/2}) + O(^3P_J)$ channel is clearly observed. The feature was not observed with either the probe or photodissociation laser blocked, either pulsed valve off, or with the probe laser tuned off-resonance. In addition, the appearance of the IO signal is sensitive to the photodissociation wavelength. At shorter photodissociation wavelengths, beyond the bandhead, the signal is lost while at longer wavelengths the anisotropy is first observed to decrease significantly before the signal is finally lost. A similar effect has been recently reported, and its origin discussed, in the case ClO photodissociation [43]. Fig. 2 shows the speed distribution (closed circles) derived from the images shown in the lower panel of Fig. 1. The upper panel shows an expanded region from 900 m/s to 1200 m/s. The two features in the speed distribution are associated with I_2 photodissociation. photodissociation [44,45]. The peak at 948 m/s is due to I_2 photodissociation at 454.9 nm to give $I(^2P_{3/2}) + I(^2P_{3/2})$ fragments. We also observe the minor $I(^2P_{3/2}) + I(^2P_{1/2})$ channel which is not shown but can be seen in the raw and reconstructed images. The peak at 1100 m/s is due to I_2 photodissociation at the probe wavelength of 304.67 nm to give $I(^2P_{3/2}) + I(^2P_{1/2})$ [46]. The FWHM of these peaks correspond to a $\Delta v/v \sim 0.03$ which is close to the instrumental resolution and these two peaks provide an accurate pixel-speed calibration of the images. The lower panel shows an expanded region to highlight the feature, centered at 240 m/s, due to IO photodissociation at 454.9 nm. The FWHM of the feature associated with the $I(^2P_{3/2}) + O(^3P_J)$ channel arising from IO photodissociation at 454.9 nm is approximately 24 m/s and is the result of several factors.

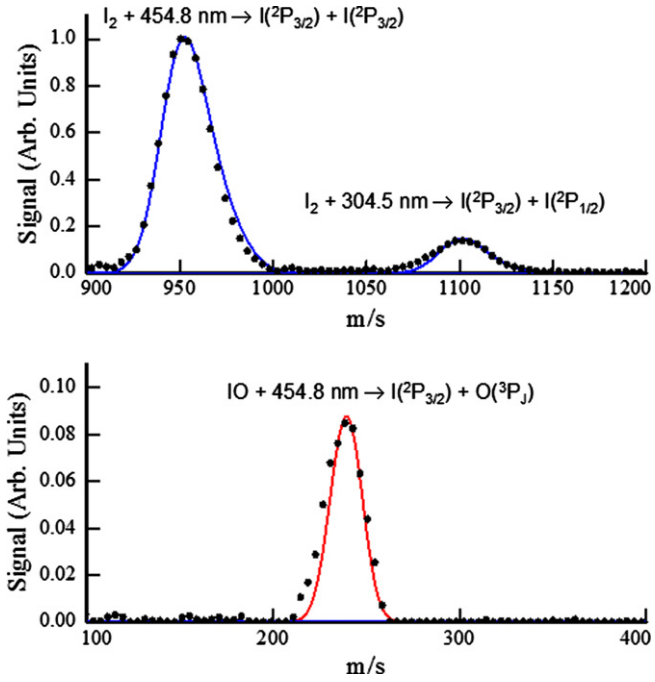

Fig. 2. Speed distributions derived from $I(^2P_{3/2})$ images with the source laser on (closed circles). For clarity the relevant regions of the speed distribution are expanded and the identities of the peaks are clearly labeled. The solid lines are forward-convolution fits to the speed distribution.

The additional kinetic energy imparted to the iodine atom due to the ionization process is 3.4 m/s [47]. It is also difficult to resolve the spin–orbit states of the coincident oxygen atoms. The effect of the unresolved oxygen fine-structure distribution will be discussed below.

In Fig. 2 the solid lines represent the forward-convolution simulation based on energy conservation,

$$h\nu + E^{IO}_{v,J,e} - D^0_0(\mathrm{IO}) = E^{\mathrm{total}}_{\mathrm{trans}} + E^{\mathrm{I}}_e + E^{\mathrm{O}}_e, \quad (3)$$

where hν is the energy of the dissociation photon, $D^0_0(\mathrm{IO})$ is the bond energy of IO, E^{I}_e and E^{O}_e are the spin–orbit energies of I and O, and $E^{\mathrm{IO}}_{v,J,e}$ is the initial internal energy of the IO radical. An assumed statistical distribution of oxygen fine-structure states, i.e. $O(^3P_2)$:$O(^3P_1)$:$O(^3P_0)$ = 0.625:0.375:0.125, provides a reasonable forward-convolution fit to the observed width of the speed distribution. We adjust a single value for the bond dissociation energy to provide the best forward-convolution fit to the $I(^2P_{3/2}) + O(^3P_J)$ channel shown as the solid line in the lower panel of Fig. 2. We find a value of 54.9 kcal/mol for the IO BDE provides the best fit to the data. The width of each spin–orbit feature was fixed as the instrumental response function broadened by the additional kinetic energy imparted from the ionization process. Our assumption of a statistical distribution of oxygen fine structure states is consistent with previous measurements of the ClO and BrO oxygen spin orbit state distributions [37,38]. If no $O(^3P_2)$ fragments were formed in the dissociation the BDE would be overestimated by approximately 0.4 kcal/mol. Iterative adjustment of the spin–orbit branching ratios to obtain the best fit provided only marginal improvement. In all cases the best fits required a dominant contribution from the $O(^3P_2)$ and lesser contributions from $O(^3P_1)$ and $O(^3P_0)$ states. Fits employing only a single oxygen spin state were markedly worse.

In the following section, we address possible sources of experimental error arising from uncertainties in IO internal energy, wavelength calibration, the pixel to speed scaling, and ionization process. We conclude that these represent minor effects in the present experiment and do not alter the reported value or error bounds. Given the resolved nature of the bound-bound transitions in the excitation step, the role of spin–orbit or vibrationally excited IO photodissociation is minimal. In addition, such initial internal energy would be resolved in the speed distribution and is not observed. Since we excite near the rotational bandhead we estimate that the parent rotational energy is <0.1 kcal/mol. Any error in the photon energy of the dissociation laser has a direct effect on the derived bond dissociation energy. The dissociation wavelength was calibrated using a Cu–Ne hollow cathode lamp. An unlikely error of 0.1 nm in the wavelength would only change the derived bond energy of IO by ± 0.02 kcal/mol. The pixel to speed scaling factor, which is critical in providing speeds from the measured images was determined accurately by fitting the data arising from I_2 photodissociation at two wavelengths using the accurate bond dissociation energy for I_2 [48]. We believe that any uncertainty caused by scaling factor is less than 0.6% leading to errors of only 1.5 m/s in the speed of I fragments associated with IO photodissociation and, therefore, a negligible difference in derived BDE. Although the $I(^2P_{3/2})$ fragment speeds are affected by excess kinetic energy imparted to the cation during the 2 + 1 REMPI process, this effect will not change the peak positions, but would only contribute to the observed width of the peaks. Given the sources of errors and the sensitivity of the measurement to the $A^2\Pi_{3/2}$ threshold we believe a conservative estimate of the uncertainty in the bond dissociation energy is $54.9^{+0.2}_{-0.4}$ kcal/mol. This value is within the error bounds of previous IO flame studies (57 ± 6 kcal/mol) [26] and molecular beam studies (53 ± 3 kcal/mol and 55 ± 2 kcal/mol) [27–29] and in excellent agreement with a more recent calculated value by Peterson of 55.2 ± 0.5 kcal/mol [49].

The photofragment angular distribution was fit according to [50]

$$I(\theta) = \frac{1}{4\pi}[1 + \beta P_2(\cos\theta)], \quad (4)$$

where β is the spatial anisotropy parameter which is +2 for a purely parallel transition ($\Delta\Omega = 0$) and −1 for a purely perpendicular transition ($\Delta\Omega = \pm 1$), $P_2(\cos\theta)$ is the second Legendre polynomial, and θ is the angle between the fragment recoil direction and laser polarization direction. Using pBASEX, we find a best-fit anisotropy parameter of 1.8 ± 0.1 for the $I(^2P_{3/2}) + O(^3P_J)$ channel. This value is consistent with the parallel $A^2\Pi_{3/2}$–$X^2\Pi_{3/2}$. In a recent article, Kim et al. studied the change in the photofragment anisotropy as a function of excitation wavelength within vibrational bands of ClO [43]. The observation of stronger anisotropy near the bandhead and more isotropic distributions for higher rotational levels was described using the treatment of Mukamel and Jortner [51]. Because the measurement anisotropy parameter for IO photodissociation in the present experiments is nearly limiting, we conclude that we are exciting near the bandhead of the 1–0 vibrational transition. This provides further confirmation of the dissociation wavelength, and increases our confidence that we are observing only the lower rotational states of IO.

4. Conclusions

We have studied the wavelength-dependent photodissociation dynamics of expansion-cooled IO radical using velocity map ion imaging. This study represents the first reported molecular beam study of the IO radical. Based on the measured photofragment speed distribution following excitation at 454.9 nm we have directly determined the ground state bond energy of IO to be $D^0_0(\mathrm{IO}) = 54.9^{+0.2}_{-0.4}$ kcal/mol. Using thermodynamic reference data for I and O ($\Delta H^{0\ \mathrm{K}}_f(O) = 58.98 \pm 0.02$, $\Delta H^{298\ \mathrm{K}}_f(O) = 59.55 \pm 0.02$, $\Delta H^{0\mathrm{K}}_f(I) = 25.61 \pm 0.01$, $\Delta H^{298\ \mathrm{K}}_f(I) = 25.52 \pm 0.01$, all values are given in kcal/mol) [52], our determined $D^0_0(\mathrm{IO})$ corresponds to a 298 K heat of formation of $\Delta H^{298}_f(\mathrm{IO}) = 29.2\ ^{+0.4}_{-0.2}$ kcal/mol. This measure-

ment reduces the uncertainty of this value and hence other thermodynamic values that rely on the IO heat of formation. We are confident that this study will aid in the improvement of atmospheric modeling particularly in the marine boundary layer where IO is especially relevant.

Acknowledgements

Support for this project was provided by the Robert A. Welch Foundation (A-1402). The authors would like to thank Professor K.A. Peterson for sharing results prior to publication. The authors acknowledge the support of the Texas A&M University Center for Atmospheric Chemistry and the Environment (CACE).

References

[1] W.L. Chameides, D.D. Davis, J. Geophys. Res. 85 (1980) 7383.
[2] R. Vogt, R. Sander, R. von Glasow, P.J. Cruzten, J. Atmos. Chem. 32 (1999) 375.
[3] T. Hoffman, C.D. O-Dowd, J.H. Seinfeld, Geophys. Res. Lett. 28 (2001) 1949.
[4] W.J. Bloss, D.M. Rowley, R.A. Cox, R.L. Jones, J. Phys. Chem. A 105 (2001) 7840.
[5] D.M. Rowley, W.J. Bloss, R.A. Cox, R.L. Jones, J. Phys. Chem. A 105 (2001) 7855.
[6] B. Laszlo, R.E. Huie, M.J. Kurylo, A.W. Miziolek, J. Geo. Res. 102 (1997) 1523.
[7] Y. Bedjanian, G. Poulet, Chem. Rev. 103 (2003) 4639.
[8] M.E. Tucceri, T.J. Dillon, J.N. Crowley, Phys. Chem. Chem. Phys. 7 (2005) 1657.
[9] T.J. Dillon, M.A. Blitz, D.E. Heard, J. Phys. Chem. A 110 (2006) 6995.
[10] B.J. Allen, J.M.C. Plane, J. Phys. Chem. A 106 (2002) 8634.
[11] E.P. Daykin, P.H. Wine, J. Phys. Chem. 94 (1990) 4528.
[12] M.H. Harwood, J.B. Burkholder, M. Hunter, R.W. Fox, A.R. Ravishankara, J. Phys. Chem. A 101 (1997) 853.
[13] C.E. Canoso-Mas, A. Vipond, R.P. Wayne, Phys. Chem. Chem. Phys. 1 (1999) 761.
[14] P. Spietz, J.C.G. Martín, J.P. Burrows, J. Photochem. Photobiol., A: Chem. 176 (2005) 50.
[15] C.E. Miller, E.A. Cohen, J. Chem. Phys. 118 (2003).
[16] S.H. Ashworth, B.J. Allan, J.M.C. Plane, Geophys. Res. Lett. 29 (2002) 1456.
[17] S.M. Newman, W.H. Howie, I.C. Lane, M.R. Upson, A.J. Orr-Ewing, J. Chem. Soc., Faraday Trans. 94 (1998) 2681.
[18] S. Himmelmann, J. Orphal, H. Bovensmann, A. Richter, A. Ladstaetter-Weissenmayer, J.P. Burrows, Chem. Phys. Lett. 251 (1996) 330.
[19] Y. Bedjanian, G. Le Bras, G. Poulet, J. Phys. Chem. A 102 (1998) 10501.
[20] R.T. Birge, H. Sponer, Phys. Rev. 28 (1926) 259.
[21] R.A. Durrie, D.A. Ramsay, Can. J. Phys. 36 (1958) 35.
[22] S. Roszak, M. Krauss, A.B. Alekseyev, H.P. Liebermann, R.J. Buenker, J. Phys. Chem. A 104 (2000) 2999.
[23] E.H. Coleman, A.G. Gaydon, W.M. Vaidya, Nature (London) 162 (1948) 108.
[24] R.B. Singh, D.K. Rai, Can. J. Phys. 43 (1965) 1985.
[25] V.M. Trivedi, B. Gohel, J. Phys. B 5 (1972) L38.
[26] L.F. Phillips, T.M. Sugden, Trans. Faraday Soc. 57 (1961) 914.
[27] D.S.A.G. Radlein, J.C. Whitehead, R. Grice, Nature 253 (1975) 37.
[28] R.J. Buss, S.J. Sibener, Y.T. Lee, J. Phys. Chem. 87 (1983) 4840.
[29] It should be noted that the value attributed to Ref. 28 is based on a footnote within the manuscript based on unpublished data from the $O(^3P) + ICl$ reaction.
[30] K.A. Peterson, B.C. Shepler, D. Figggen, H. Stoll, J. Phys. Chem. A 110 (2006) 13877.
[31] N. Kaltsoyannis, J.M.C. Plane, Phys. Chem. Chem. Phys. 10 (2008) 1723.
[32] Y. Bedjanian, G. LeBras, G. Poulet, J. Phys. Chem. A 101 (1997) 4088.
[33] H.F. Davis, Y.T. Lee, J. Chem. Phys. 105 (1996) 8142.
[34] N. Taniguchi, K. Takahashi, Y. Matsumi, S. Dylewski, J. Geiser, P.L. Houston, J. Chem. Phys. 111 (1999) 6350.
[35] A.V. Komissarov, M.P. Minitti, A.G. Suits, G.E. Hall, J. Chem. Phys. 124 (2005) 014303.
[36] E. Wrede, S. Laubach, S. Sculenburg, A.J. Orr-Ewing, M.N.R. Ashfold, Chem. Phys. Lett. 326 (2000) 22.
[37] H. Kim, K.S. Dooley, E.R. Johnson, S.W. North, J. Chem. Phys. 124 (2006) 134304.
[38] H. Kim, J. Park, T.C. Niday, S.W. North, J. Chem. Phys. 123 (2005) 174303.
[39] H. Kim, K. Dooley, E. Johnson, S.W. North, Rev. Sci. Instrum. 76 (2005) 124101.
[40] S.M. Newman, W.H. Howie, I.C. Lane, M.R. Upson, A.J. Orr-Ewing, J. Chem. Faraday Trans. 94 (1998) 2681.
[41] C.E. Moore, Atomic Energy Levels, Natl. Stand. Ref. Data Ser., Natl. Bur. Stand. U.S. Circ 35, vol. 3, U. S. Government Printing Office, Washington, DC, 1971;
Y.J. Jung, Y.S. Kim, W.K. Kang, K.H. Jung, J. Chem. Phys. 107 (1997) 7187.
[42] G.A. Garcia, L. Nahon, I. Powis, Rev. Sci. Instrum. 75 (2004) 4989.
[43] H. Kim, K.S. Dooley, S.W. North, G.E. Hall, P.L. Houston, J. Chem. Phys. 125 (2006) 133316.
[44] H.J. Hwang, M.A. El-Sayed, J. Phys. Chem. 95 (1991) 8044.
[45] D.A. Chestokov, D.H. Parker, K.V. Vidna, T.P. Rakitzis, J. Chem. Phys. 124 (2006) 024315.
[46] The very minor $I(^2P_{3/2}) + I(^2P_{3/2})$ from dissociation at 304.67 nm can also be observed at higher extraction voltages.
[47] B. Whitaker, Imaging in Molecular Dynamics, Cambridge University press, New York, 2003.
[48] R. Atkinson, D.L. Baulch, R.A. Cox, R.F. Hampson, J.A. Kerr, M.J. Rossi, J. Troe, J. Phys. Chem. Ref. Data 29 (2000) 167.
[49] K. A. Peterson, 2008, unpublished data.
[50] R.N. Zare, Mol. Photochem. 4 (1972) 1.
[51] S. Mukamel, J. Jortner, J. Chem. Phys. 61 (1974) 5348.
[52] M.W. Chase Jr., C.A. Davies, J.R. Downey Jr, D.J. Frurip, R.A. McDonald, A.N. Syverud, J. Phys. Chem. Ref. Data 14 (1985) 1.